Duclos *et al.*
Translational Medicine Communications (2023) 8:4
https://doi.org/10.1186/s41231-023-00136-w

Translational Medicine Communications

RESEARCH

Open Access

Cervical catheter placement leads to improved rostral distribution of a radiolabeled 18F-baclofen analog in cynomolgus monkeys

Brian A. Duclos[1*], Cindy Roegge[1], Howard Dobson[2], Scott Haller[3], Jeff Bodner[1], Sanjana Pannem[2], Janelle Gesaman[3] and Amin Nourmohammadi[1]

Abstract

Background Intrathecal (IT) catheter delivery of baclofen via continuous infusion using an implantable pump is an important means of treating patients with severe spasticity. We evaluated the impact of IT catheter tip placement (upper vs. lower) on brain and spine distribution of a radioactive tracer molecule.

Methods Cynomolgus monkeys were implanted with an IT catheter, with the distal tip located at either C1 or T10 and attached to an implanted continuous infusion pump. A radioactive tracer molecule, an ^{18}F-baclofen analog, and PET imaging were utilized to observe tracer distribution and quantitate levels of tracer in both the brain and spine according to catheter tip location.

Results It was consistently determined that a high cervical (C1) catheter tip placement resulted in both more rapid distribution and higher concentrations of radiotracer in the brain and upper spine compared with lower thoracic (T10) during the first 6 hours of infusion.

Conclusions These results indicate that delivery of ^{18}F-baclofen by IT catheter results in repeatable proportional distribution within regions of the brain and spine. The data also suggest that the greatest exposure to the brain and cervical spinal cord occurs when the catheter tip is located at the first cervical vertebra.

Keywords Intrathecal, PET imaging, Non-human primate, Catheter, Continuous infusion pump, Baclofen, Spasticity, Distribution, Cerebrospinal fluid

Background

Intrathecal (IT) catheter delivery of baclofen via continuous infusion using an implantable pump is an important means of treatment for patients with severe spasticity, both of cerebral and spinal origin [1]. Although catheter tips are most commonly placed in the thoracic spine [2], an alternative placement of the tip may be necessary for a variety of reasons, including complicated spinal anatomies that may occur with scoliosis or spinal fusions [3]. Several studies have been performed to understand the clinical implications to treatment efficacy as a result of alternative placement [2, 4–18] as well as the effect of cerebrospinal fluid (CSF) concentration of baclofen as a result of varied catheter tip location [19]. However, to date there have been no studies to examine the

*Correspondence:
Brian A. Duclos
brian.a.duclos@medtronic.com
[1] Medtronic, 7000 Central Ave NE, Minneapolis, MN 55432, USA
[2] Invicro, 119 4th Avenue, Needham, MA 02494, USA
[3] Charles River Laboratories, 54943 N Main St, Mattawan, MI 49071, USA

effect of catheter tip placement on brain distribution of baclofen, which could be an important factor for patients with spasticity of a cerebral origin based on bolus lumbar puncture test observations in patients with spasticity of a cerebral origin performed by Richard et al. [16]. Additionally, region-specific brain concentrations have implications for therapy efficacy in other neurological disorders [20–23].

Distribution to central nervous system (CNS) tissues via the CSF largely relies on several convective forces such as CSF turnover, respiration, cardiac motion, and body movement that all contribute to the pulsatile flow [24–27]. However, when utilizing IT drug delivery via an implantable infusion system, multiple factors such as concentration, volume, and rate of infusion can also contribute to the overall distribution [28]. Most recently, the ability of a large volume IT bolus injection of recombinant enzyme via an implanted catheter has been shown to facilitate improved distribution to the brain parenchyma as well as the neurons of the brain and spinal cord equivalent to an implanted intracerebroventricular (ICV) catheter in both dogs and cynomolgus monkeys [29–31]. Similar volume effects were observed in the IT bolus injection of both antisense oligonucleotides and radiotracers in cynomolgus monkeys via lumbar puncture [32, 33].

To better understand the effect of catheter tip placement on distribution to the CNS tissues in a larger species, in particular the brain and cervical spine, a therapeutically relevant ^{18}F-baclofen analog with comparable binding affinity to baclofen was synthesized to facilitate positron emission tomography (PET) imaging in non-human primates [34]. Note that the infusion system used for this study is FDA-approved for delivery of intrathecal baclofen but not specifically for the ^{18}F-Baclofen analog in this study. A flow rate corresponding to a monthly refill interval for a 40-mL implantable pump (55 µL/hr) was selected, and infusate was delivered continuously over a 6-hour interval at two different catheter positions (C1 and T10) with continuous image acquisition. Images produced from the two catheter tip positions were mapped to the Invicro proprietary non-human primate (NHP) brain atlas, and region-specific concentrations were assigned.

Methods

Continuous infusion system implant procedure

Three young, adult male cynomolgus monkeys were used in the study. Monkeys were 63–69 months of age and 5.1-6.2kg body weight at implant. The in vivo portion of the study was executed at Charles River Laboratories Mattawan, Michigan. Under routine general anesthesia, and following aseptic procedures, an intrathecal catheter (Medtronic Ascenda™ 8781) was introduced in the intrathecal space at the articulation of the second and third lumbar vertebrae, with the catheter tip located at the level of the first cervical vertebra (C1). During the same procedure, a delivery pump with a 20-mL reservoir (SynchroMed™ II 8637-20) was placed in the abdominal cavity, and the intrathecal catheter was connected by tunneling through the subcutaneous tissue. Following the first imaging procedure, the tip of the catheter was repositioned to the level of the tenth thoracic vertebra (T10). The length of the trimmed catheter was recorded at the time of each surgery. A minimum of 10 days were allowed for healing to occur between surgery and imaging to ensure that there were no leaks at the site at which the catheter penetrated the meninges. Immediately following surgery, the pump reservoir was loaded with preservative-free normal saline, and the pump was programmed to deliver 0.05 mL/day to maintain catheter patency. The two conditions under which the imaging was conducted are referred to as C1, where the catheter tip was placed at the first cervical vertebra and T10, where the catheter tip was located at the tenth thoracic vertebra.

PET imaging study design

The ^{18}F Baclofen labelling was based on the method described by Naik et al. [35]. Chemical and radiochemical purity was determined using standard HPLC methods. Imaging was performed under routine general anesthesia. On the day of imaging, the preservative-free saline was removed from the pump reservoir by syringe and replaced with 1.5–6.2 mCi of ^{18}F-Baclofen in 1.5 mL phosphate-buffered saline. The pump was programmed to deliver the required volume (priming bolus) to displace the normal saline in the catheter over a 30-minute period and then programmed to deliver the ^{18}F-Baclofen at a rate of 1.332 mL/day (0.055 mL/h) for a period of 6 hours. Whole body PET images (Siemens microPET Focus 220) were acquired for the full 6-hour period starting immediately prior to the delivery of the ^{18}F-Baclofen. Images were acquired in list mode and subsequently processed into 5-minute bins for later analysis. A whole-body CT (Neurologica CereTom OtoScan) image was acquired on completion of the PET imaging for anatomical localization of the radioactivity and attenuation correction of the PET data. The ^{18}F-Baclofen delivery and image acquisition was identical for the two imaging sessions before and after repositioning of the catheter tip.

Reconstructed PET and CT were coregistered and resampled to 0.6 mm^3 voxels that were scaled to µCi per voxel based on a phantom filled with a known

concentration of ^{18}F that was included in the image. Brain regions of interest (ROI) were generated by registering Invicro's 42 region NHP brain atlas to the *in vivo* brain data based on the CT image using VivoQuant tools. Spinal cord plus CSF ROIs were generated to encompass all activity within the spinal canal. These were divided into four subregions: cervical, upper thoracic, lower thoracic, and lumbar. Cervical spinal cord, upper thoracic spinal cord, lower thoracic spinal cord, and lumbar spinal cord ROIs were generated by eroding the corresponding 'spinal cord + CSF' ROIs by 1 pixel to exclude the CSF. Liver ROIs were defined by placing spheres in the corresponding anatomical locations based on either PET uptake when present or the appropriate anatomical region on the CT image when absent. Kidney ROIs consisted of whole organ phantoms placed in their corresponding anatomical locations based on CT and PET uptake where present. Bladder ROIs were segmented to encompass all activity within the tissues. In cases where no activity was evident in the region, the region was defined by placing one spherical volume in the corresponding anatomical location. The uptake and area under the curve (AUC) of the ^{18}F-Baclofen at each time point for each ROI generated was determined. The AUC was calculated for each ROI using the trapezoidal method (with no uptake at time 0 hour) and plotted in units of μCi-min. For the brain regions, the mean value for the AUC for each region under each condition was calculated and the ratio of the two values determined. Finally, data from each anatomical region were binned based on the exposure to each region to create a map of the distribution of the ^{18}F-Baclofen.

PET data statistical analysis

The pharmacokinetics of the tracer in different ROIs in the brain was studied with a 5-min time resolution during the span of 6 hours; PET data were collected in three 2-hour block time series due to volume of data being collected. The recorded time series were then analyzed (both within each subject and across the cohort) to identify the presence of temporal and spatial distribution patterns across different ROIs. In the first step, the concentration of the radiotracer was used to calculate the final uptake value for each ROI at the end of the scan (T = 6h). The concentration values were then normalized and sorted within each group (C1 vs T10) to investigate whether the pharmacokinetics within each group is time-invariant or not. A heuristic 'similarity index (SI)' (ranging from 0, indicating lack of any similarity, to 100 indicating complete overlap) was used to understand whether within subjects' observations can be generalized across the cohort by comparing the final uptake value between pairs of subjects (i.e. subject 1 vs 2, subject 1 vs 3, and subject 2 vs 3) within each group. In another inter-subject analysis, each ROI was studied and the similarity in the time series was evaluated with that ROI across different subjects. The area under the curve (AUC) for each of the three time series associated with individual ROIs in each subject were compared.

Results

In general, all subregions of the brain showed progressive accumulation of radioactivity over time. Data for the hippocampus are presented in Fig. 1. The total activity that accumulated in the brain was markedly higher and occurred sooner with the catheter tip placed at C1

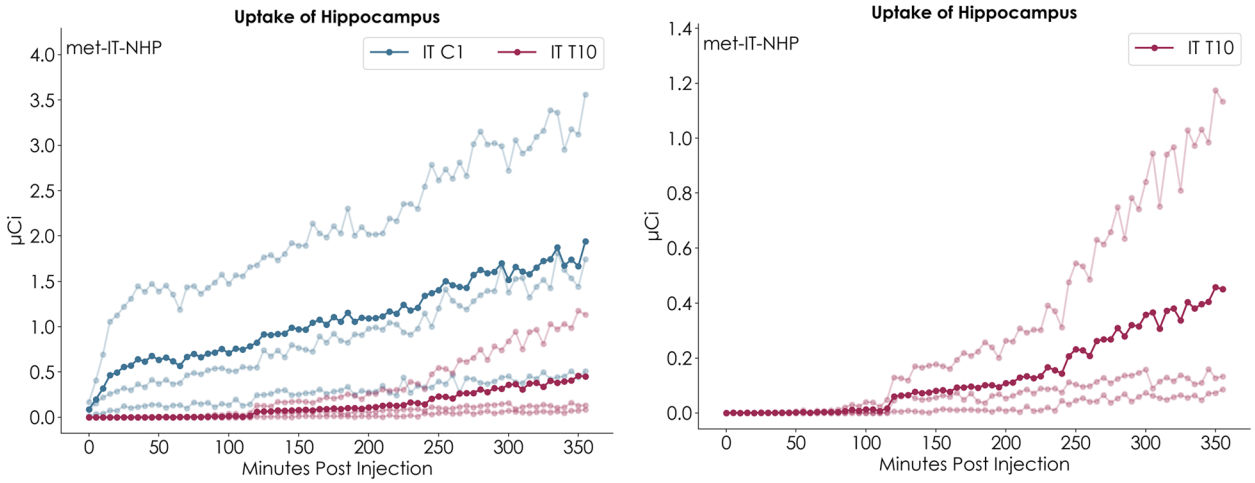

Fig. 1 Time activity curves for the hippocampus. The left plot has data for both catheter tip at C1 (blue) and catheter tip at T10 (red). The darker color represents the mean of the 3 subjects each represented by the lighter color. The right plot presents the data for catheter tip at T10 only, with a different y-axis scale, highlighting some individual animal variation in distribution

compared to the catheter tip at T10 (Fig. 2). With the catheter tip at C1, radioactivity was identified in portions of the brain within the first 5 minutes of imaging. However, in very small, deeper areas, such as the anterior putamen, no significant activity was detected for at least 2 hours, and as might be expected, the data are noisier. Data for all regions are presented in Figs. 1–51 in the Supplemental Data.

The ratio of the uptake under the two catheter tip placements (C1:T10) demonstrated marked variation, ranging from a high of 53.67 for the limbic cingulate cortex to a low of 4.07 for the fusiform gyrus and a mean of 14.76 (Table 1). Additional tabulated data are presented in the Supplemental Data for the brain and spine exposure to ^{18}F-baclofen as the raw data, ratios of exposure between the C1 and T10 catheter tip locations, and coefficient of variance in Tables 1 and 2, respectively. The exposure to ^{18}F-baclofen in each region for the brain and spine, expressed as μg-min, are presented in Supplemental Tables 3 and 4, respectively. The radioactivity distribution map is presented in Fig. 2. The highest exposure to the ^{18}F-Baclofen is in the periphery of the brain and adjacent to the falx cerebri where the brain parenchyma is immediately adjacent to the CSF. No immediately discernable pattern of distribution throughout the brain parenchyma could be identified which may be due to multiple factors contributing to brain distribution (e.g. centripetal distribution or distribution along perivascular or periventricular routes). The implication of this is that the distribution is not based on simple diffusion and that an active process is likely to be involved, the magnitude of which varies through the brain (Fig. 3).

For the spinal cord (Table 2), a higher catheter tip placement resulted in more distribution to the cervical and upper thoracic spine as demonstrated by a high ratio (C1:T10) of the AUC for the cervical spine (15.47) and the upper thoracic spine (2.5). However, distribution to the lower thoracic and lumbar spine were similar with

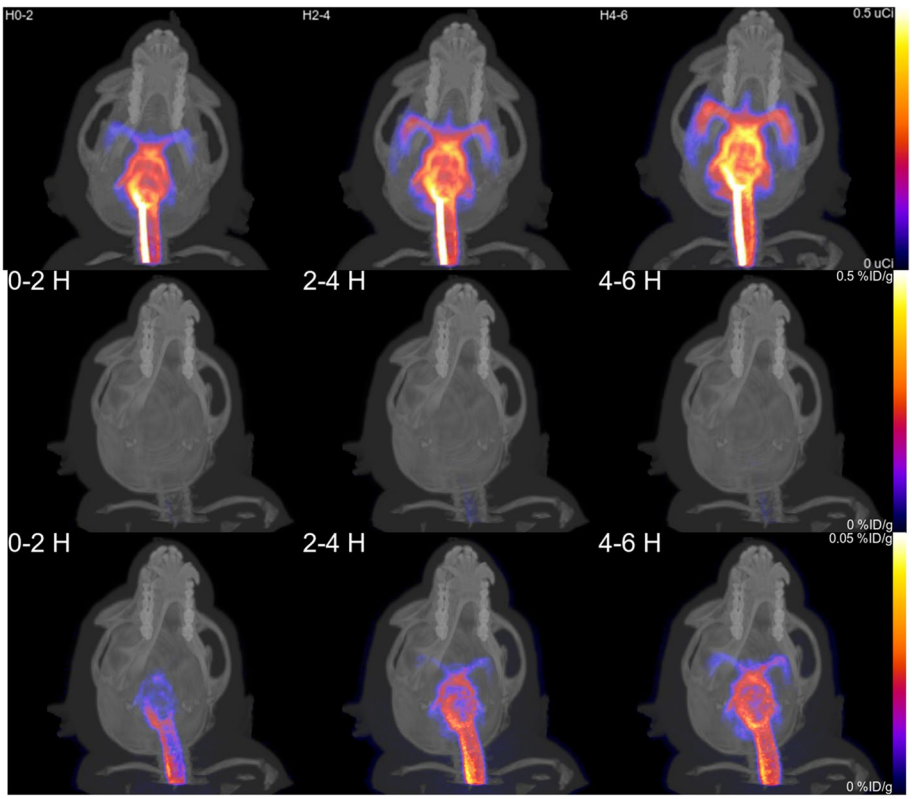

Fig. 2 Summed images acquired at 0–2, 2–4 and 4–6 hours following the start of administration with the catheter tip at the first cervical vertebra (C1) (top) and the tenth thoracic vertebra (T10) (middle) demonstrating the delayed distribution within the brain following delivery in the thoracic spine compared to the cervical spine. The color scale is identical for the top and middle panels (0-0.5% ID/g). The bottom panel is the same figure as the middle panel but with a different color scale (0-0.05% ID/g) demonstrating that activity is present in the brain, but in lower amounts. The low intensity in the middle panel demonstrates that there is much less activity in the brain with the T10 catheter placement and that the low tracer distribution was potentially offset by clearance rates. We used the same color scale for the top and middle panels in order to illustrate this marked difference. To demonstrate that there is indeed radioactivity in the middle panel, the color scale for the bottom panel has been changed to a range that demonstrates the lower activity (0-0.05% ID/g)

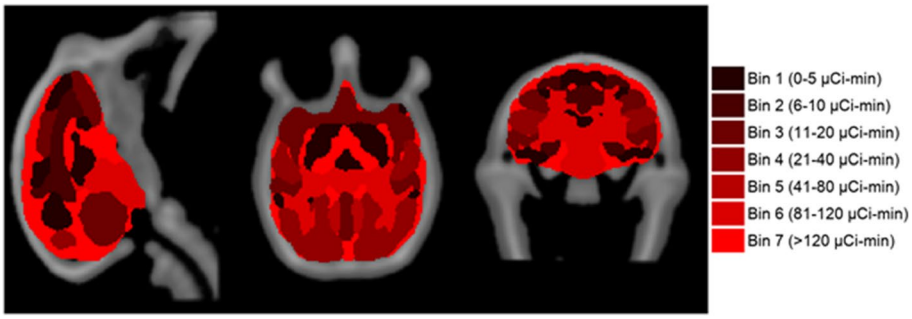

Fig. 3 Representative image of the mean AUC distribution throughout the brain

either catheter tip location (0.94 and 0.88, respectively, for C1:T10 ratio).

Additionally, our analysis showed that the averaged SI value for group C1 (71%) was two-fold larger than its counterpart for group T10 (35%), which is a clear indication that the consistency of pharmacokinetics in the first group (C1) is significantly higher than the second group (T10). This inter-group difference also manifests in the cross-correlation analysis between the time series associated with different ROIs within each group (Fig. 4). A comparison between the Pearson correlation coefficients between the two confusion matrices in this figure is another compelling evidence that the inter-subject similarity within the first group (Fig. 4, pane A) is higher than in group 2 (Fig. 4, pane B).

Discussion

This study was performed in a continued effort to understand the inputs that drive therapy enhancement using an implantable IT drug delivery solution. The objective of this NHP work is to be able to augment current clinical research on catheter placement in IT baclofen therapy by providing additional understanding of the efficacy observations in clinical practice [17–19] as well as provide a means to increase the cranial distribution of IT delivered therapeutics. Previous studies in rhesus NHPs showed brain distribution of gadolinium-labeled diethylenetriamine pentaacetate (DTPA, MW 600 Da) as a surrogate for small molecules and gadolinium-labeled albumin (MW 74,000 Da) as a surrogate for peptides and mid-size biologics with both IT and ICV continuous infusion via a catheter and infusion pump. In these studies, global brain and spinal cord distribution was visualized by MRI imaging, but any further quantification of the data was challenging. This previous study also demonstrated that a minimal IT infusion rate of 0.4 mL/day was needed to achieve brain distribution whereas a lower infusion rate of 0.1 mL/day resulted in very limited brain distribution of the gadolinium-labeled compounds with MRI imaging [36].

The inherent capabilities of an implanted programmable drug infusion pump such as flow rates, and thus infusate volume, can be exploited to drive rostral delivery. Indeed, in a previous experiment in our laboratories, both benchtop and *in silico* modeling demonstrated that CSF oscillations are a larger driving force to rostral CSF distribution than infusion rate alone, even at the maximum rate of an infusion pump. It was also noted that increasing the total volume of a bolus, as in therapy trialing, can impact the degree of mixing observed more than possible rate adjustments with an infusion pump [37]. However, this current study shows that the placement of the catheter tip at the time of implant may have the most profound effect. Although the ability to manage spasticity is excellent with current clinical practices, it is important to understand the implications of changing this surgical implant parameter. In addition to spasticity, there are a variety of indications where enhanced distribution to key regions of the brain would be of value and potentially offer an alternative and less invasive solution to ICV catheterization. As clinicians consider the best treatment options for their patients, it is critical to understand both the opportunities and limitations of various drug delivery solutions. Conversely, it may be beneficial to maintain a lower, thoracic placement of the catheter tip for indications where a more local, less rostral spread of the therapeutic is desired.

In this experiment, with respect to brain concentrations, we observed the greatest difference in distribution (absolute exposure as well as pharmacokinetic patterns) between catheter tip positions in the posterior regions of the NHP brain, including the cerebellum and cerebellar white matter, brain stem, amygdala, insula, posterior putamen, and anterior and limbic cingulate cortex, with a maximum average C1:T10 AUC

Table 1 Mean tracer concentrations by grouped brain regions and ratio of concentrations by catheter tip level

Brain Region	Mean (μCi*min)		Ratio C1/T10
	C1	T10	
Rest of Brain[1]	153.4	11.2	13.67
Brain Stem	112.6	5.3	21.30
Cerebellum	77.8	4.7	16.49
Cerebellar White Matter	22.2	0.8	27.82
Vermis	14.2	1.4	10.48
Occipital Cortex	39.8	4.2	9.56
Amygdala	21.2	0.8	25.86
Anterior Cingulate Cortex	8.5	0.2	39.64
Posterior Cingulate Cortex	5.7	0.3	16.60
Limbic Cingulate Cortex	1.6	0.0	53.67
Orbitofrontal Cortex	12.7	0.9	13.50
Dorsolateral Frontal Cortex	1.5	0.2	6.21
Medial Frontal Cortex	0.7	0.1	10.05
Ventral Frontal Cortex	1.9	0.3	6.10
Precuneus	2.5	0.3	9.32
Premotor Cortex	13.2	1.4	9.24
Primary Motor Cortex	2.8	0.4	7.97
Primary Sensory Cortex	8.2	0.9	9.46
Superior Parietal Cortex	2.7	0.4	7.13
Inferior Parietal Cortex	11.7	0.9	12.42
Insula	14.3	0.4	37.90
Medial Temporal Cortex	11.1	1.2	9.13
Superior Temporal Cortex	33.9	2.1	16.14
Hippocampus	6.4	0.8	7.76
Fusiform Gyrus	4.0	1.0	4.07
Entorhinal Cortex	2.9	0.2	15.78
Inferior Temporal Cortex	3.5	0.6	6.05
Parahippocampal Gyrus	6.4	0.5	13.32
Anterior Caudate Nucleus	2.2	0.1	15.21
Posterior Caudate Nucleus	0.5	0.1	7.89
Anterior Putamen	3.7	0.2	16.25
Posterior Putamen	4.5	0.2	20.95
Ventral Posterior Putamen	0.9	0.1	9.10
External Pallidum	0.8	0.1	11.38
Internal Pallidum	0.4	0.0	11.67
Ventral Striatum	3.0	0.1	21.64
Substantia Nigra	1.2	0.1	12.24
Thalamus	2.0	0.2	7.97
Lateral Ventricle	1.5	0.2	8.33
Third and Fourth Ventricles	1.8	0.2	11.31

[1] Rest of the brain includes all brain tissue not included in the specified regions

Table 2 Mean tracer concentrations by spinal region and ratio of concentrations by catheter tip level

Spinal Cord Region	Mean (μCi*min)		Ratio C1/T10
	C1	T10	
Cervical	84.0	5.4	15.47
Upper Thoracic	16.8	6.7	2.50
Lower Thoracic	88.3	94.3	0.94
Lumbar	71.5	81.1	0.88
Cervical + CSF	252.1	12.1	20.88
Upper Thoracic + CSF	106.7	21.4	5.00
Lower Thoracic + CSF	178.9	219.5	0.82
Lumbar + CSF	166.1	165.0	1.01
Whole body[1]	70,999	54,881	1.29

[1] The whole body includes the residual radioactivity in the image that is not included in the spinal cord or CSF regions

ratio of 39.6 for the anterior cingulate cortex. On average, the C1:T10 AUC ratio was found to be 14.8. The highest overall exposures were achieved for the cerebellum, brain stem, amygdala, occipital cortex, and the superior temporal cortex. Therefore, indications where these regions are the focus of pharmacological therapy could potentially stand to benefit the most from a higher catheter tip position instead of a typical thoracic implant. Likewise, cervical catheter placement could potentially result in more consistent therapy outcomes between subjects if the intended target was located in the brain. However, the individual pharmacokinetics of each therapeutic would need to be assessed to fully understand the drug distribution to a target region, and thus potential for therapy efficacy.

Similarly, cervical and upper thoracic AUCs were much higher for C1 positioning relative to T10 tip locations. In indications such as spasticity, in particular spasticity of a cerebral origin, increased rostral distribution with C1 positioning may improve therapy outcomes from intrathecal baclofen therapy. Grabb, et al observed a mild improvement in upper limb spasticity in pediatric patients by utilizing a midthoracic catheter tip positioning (T6-7) compared to T12 positioning, highlighting the potential of alternative tip locations [4]. A retrospective review of adult spasticity patients by McCall and MacDonald showed similar improvements in mean spasticity scores with cervical tip placement over thoracic [6]. Furthermore, Adesinasi examined the effect of catheter tip location on upper and lower extremity hypertonia using the Modified Ashworth Scale and found that patients with spasticity of a cerebral origin exhibited greater improvements with tip placement at higher spinal levels than patients with spasticity of a spinal origin [9]. In addition, if it was clinically desirable to target the upper spine, it could potentially be feasible to use a lower dose to achieve the desired clinical endpoint by exploiting the improved rostral distribution to the cervical and upper thoracic regions.

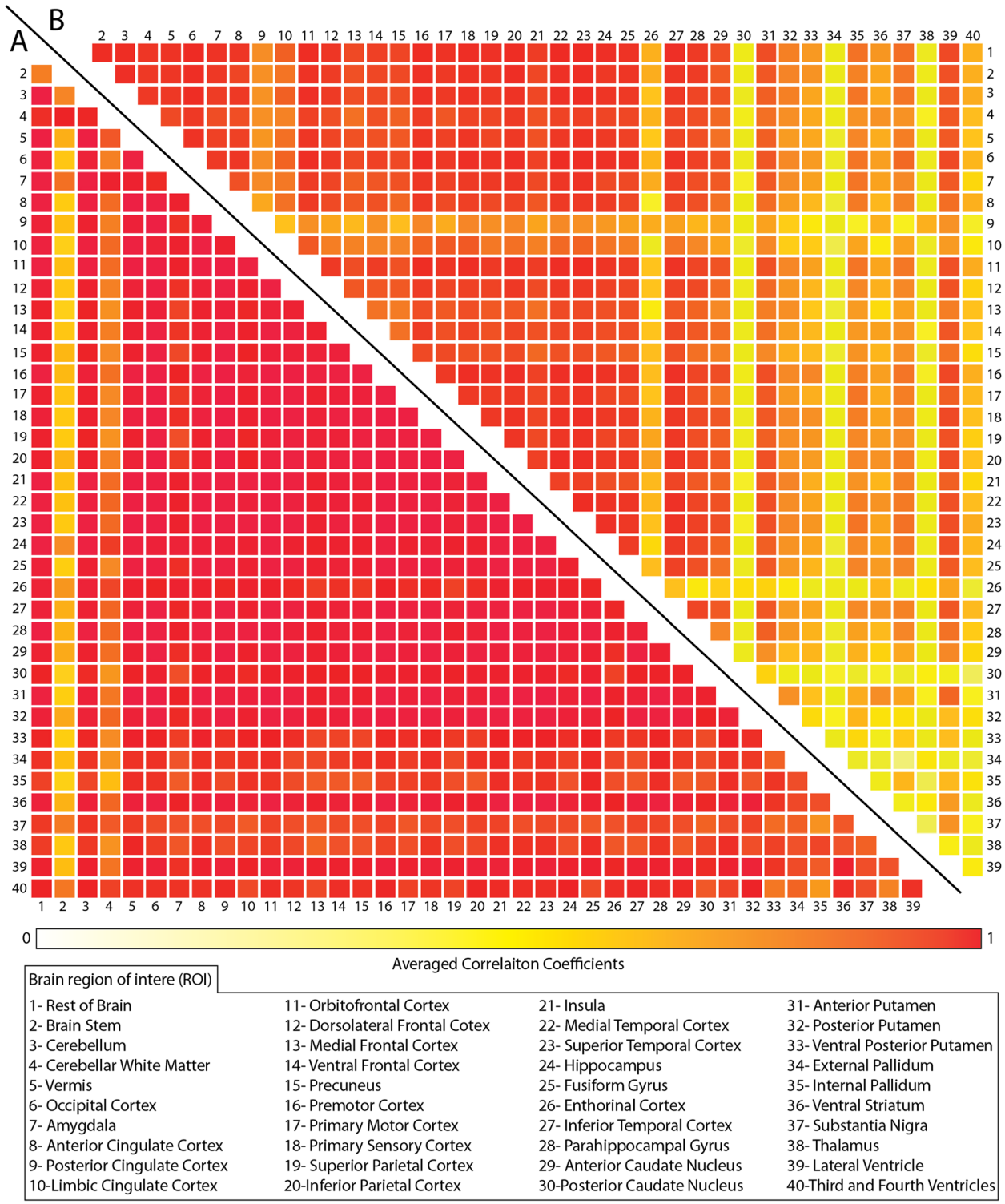

Fig. 4 Confusion matrix analyzing the time and concentration variability of the pharmacokinetics of various brain regions when the catheter tip is placed at C1 (**A**) or T10 (**B**). Each matrix demonstrates the average value across the cohort and the color bar represents the Pearson correlation coefficients. Due to the symmetric nature of the cross-correlation analysis between ROI-pairs, the lower half of each matrix was not included. A value of 1 along the x-axis denotes regions of highest similarity, while a value of 0 denotes regions of least similarity

The delivery of therapeutics by the IT route is an active area of research. A question that is currently not well answered is an explanation of the high degree of variability in uptake within different regions of the brain as well as between subjects [33]. We have seen this effect in multiple studies and as yet, we do not have a rational explanation. We also know that on repeat experiments the differences are not always consistent within a single subject. The mean coefficient of variance for the brain regions for the C1 and T10 catheter tip positions was 76% and 84%, respectively, despite marked differences in the total exposure of each region to the ^{18}F-Baclofen. The higher variability in brain distribution with the T10 catheter tip position suggests that because the ^{18}F-Baclofen has to traverse a longer length of the spinal IT space there is increased turbulence in the flow resulting from spinal nerve roots which perturbs the overall cranial flow of the ^{18} F-Baclofen.

The exposure to ^{18}F-Baclofen in the cervical spinal cord was greater with a C1 catheter tip position compared to the T10 catheter tip position by a factor of 15 in the cervical spinal cord and 2.5 in the upper thoracic spinal cord but was close to unity in the lower thoracic and lumbar spinal cord. There was also greater variability in exposure in the cervical and upper thoracic spinal cord with the T10 catheter tip placement compared to the C1 (Coefficient of Variance 31% and 55% for the cervical and upper thoracic cord for C1 catheter tip and 145% and 140% for T10 catheter tip). It is known that the driving force for CSF circulation is primarily pulsations of the arterial supply to the brain within the IT space. The pulse wave magnitude decreases as it flows down the spinal IT space, and it increases as it returns cranially [38]. The spinal cord is eccentrically placed in the spinal IT space with its position changing along the length of the spinal cord, resulting in a spiral flow of CSF in both caudal and cranial directions [39]. The data presented here indicate that the highest exposure to the cervical and upper thoracic spinal cord occurs when the tip of the catheter is located at C1, resulting in a primarily caudal flow of ^{18}F-baclofen, in contrast to the catheter tip being placed at T10 where the flow of ^{18}F-baclofen is in a rostral direction. This has implications for the therapeutic delivery of baclofen using IT catheters.

The assumption that rostral distribution as a function of catheter tip placement is consistent from NHP to human has yet to be tested beyond spinal CSF sampling [17, 19]. It may also be crucial in determining differences in intrathecal dynamics in different disease states, for instance where integrity to the blood brain barrier is diminished, including chronic neuroinflammatory disorders of the CNS such as multiple sclerosis [40]. Additionally, a better understanding of the CSF and interstitial fluid exchange along the brain-wide network of perivascular spaces, which has been termed the 'glymphatic system,' will be crucial as dysfunction of this network is a feature of the aging and injured brain and has potential implications on how therapeutics reach their desired brain targets [41]. Likewise, there certainly could be radiotracer diffusion both within the brain and the spinal cord, however this study was not designed to investigate this. There is certainly distribution within the brain tissue, but this is known to occur by a variety of mechanisms, including diffusion. This study investigated the biodistribution at a more macroscopic level. The choice of flow rate and drug volume administered for IT delivery to the brain is complex, and many different permutations have been published. The dynamics of CSF flow in the spinal CSF space are complex [42]. Largely, there are two approaches. The first is a bolus injection which, in theory, overwhelms the normal physiology resulting in the injectate volume being driven towards the brain. The second approach is a slow infusion which utilizes the normal physiology to transport the injectate to the brain, and simultaneously minimizes any perturbations of the normal flow. Logically, the delivery rate should be equal to, or lower than the normal flow rate. Published data indicate that the flow rate varies with both the site of measurement and the measurement technique. Khani et. al. demonstrated a peak CSF flow rate of 0.3-0.6mL/s in the mid cervical region in cynomolgus monkeys [43], whereas McCully et. al., determined the rate of CSF flow in rhesus monkeys using inulin administered in the lateral ventricles and sampled at the lumbar spine to be 0.018 mL/min [44]. This implies that our rate of administration of 0.055 mL/h, with good delivery to the brain, is likely to be less than the actual physiological flow rate and therefore unlikely to perturb the normal flow dynamics. Similarly, the rate could easily be translated from non-human primates to human subjects.

Conclusions

Our results suggest that delivery of ^{18}F-baclofen by spinal IT catheter results in repeatable proportional distribution within regions of the brain and confirms the findings from other studies that the total exposure of the brain varies between subjects. The data also indicate that the greatest exposure to the cervical spinal cord occurs when the catheter tip is located at the first cervical vertebra. Clearly, the conclusions are constrained by the small number of subjects but are sufficiently encouraging that further investigation is justified. At the same time, the data reaffirm the need for investigation of the inter-subject variability of the total brain exposure resulting from IT delivered therapeutics.

Abbreviations

IT	Intrathecal
CSF	Cerebrospinal fluid
ALS	Amyotrophic lateral sclerosis
CNS	Central nervous system
ICV	Intracerebroventricular
PET	Positron emission tomography
NHP	Non-human primate
CT	Computed tomography
HPLC	High-performance liquid chromatography
ROI	Region of interest
AUC	Area under the curve
µCi	Micro Curie
DTPA	Diethylenetriamine pentaacetate
MW	Molecular weight
Da	Dalton
MRI	Magnetic resonance imaging

Supplementary Information

The online version contains supplementary material available at https://doi.org/10.1186/s41231-023-00136-w.

Additional file 1.

Acknowledgments

The authors would like to acknowledge the scientists, staff, and technicians at Charles River Laboratories and Invicro for their precise execution of the studies described in this paper. The authors would like to specifically thank Dr. Wendy Marriner, and Randy Pielemeier from Charles River Laboratories and Surabhi Nair, Mark Aldridge, Dr. Vince Carroll, Jack Heimann, and Andrew Novicki from Invicro for their hard work and dedication to the project management of the imaging studies. The authors would also like to thank Dr. Linda Page and Dr. Michael Turner for their assistance in protocol review and Thomas Keene for his assistance with remotely training Charles River Laboratories staff with device programming.

Authors' contributions

BAD, CR, and HD assisted in designing the experiments and analyzed data and are co-primary authors of the manuscript. SH and JG conducted experiments, collected, analyzed data. JB assisted in designing experiments. HD assisted in writing the manuscript and interpreting the data. SP and AN assisted in analyzing the data. All authors read and approved the final manuscript.

Funding

The research described herein was wholly funded by Medtronic.

Availability of data and materials

The datasets used and/or analyzed during the current study are available from the corresponding author on reasonable request.

Declarations

Ethics approval and consent to participate

The 18F-baclofen experiment in the monkey was performed at Charles River Laboratories International, Inc. and the study procedures were reviewed and approved by the Institutional Animal Care and Use Committee at Charles River Laboratories International, Inc. prior to the start of the study. The 18F-baclofen study was performed under approved protocol 2579-094. The study complied with the U.S. Department of Agriculture's Animal Welfare Act (9 CFR Parts 1, 2, and 3) and the Guide for the Care and Use of Laboratory Animals, Institute of Laboratory Animal Resources, National Academy Press, Washington, D.C., 2011. Charles River Laboratories International, Inc. is accredited by the Association for Assessment and Accreditation of Laboratory Animal Care (AAALAC).

Consent for publication

Not applicable.

Competing interests

BAD, CR, JB, and AN are employees of Medtronic. Both CR and JB are stockholders of Medtronic as well. HD is an independent consultant contracted to Invicro, and SP is an employee of Invicro. SH is an employee of Charles River Laboratories.

Received: 29 August 2022 Accepted: 1 February 2023
Published online: 09 February 2023

References

1. Saulino M, Ivanhoe CB, McGuire JR, Ridley B, Shilt JS, Boster AL. Best Practices for Intrathecal Baclofen Therapy: Patient Selection. Neuromodulation. 2016;19(6):607–15.
2. Boster AL, Bennett SE, Bilsky GS, et al. Best practices for intrathecal baclofen therapy: screening test. Neuromodulation. 2016;19(6):616–22.
3. Scannell B, Yaszay B. Scoliosis, spinal fusion, and intrathecal baclofen pump implantation. Phys Med Rehabil Clin N Am. 2015;26(1):79–88.
4. Grabb PA, Guin-Renfroe S, Meythaler JM. Midthoracic catheter tip placement for intrathecal baclofen administration in children with quadriparetic spasticity. Neurosurgery. 1999;45(4):833–7.
5. Albright AL, Barron WB, Fasick MP, Polinko P, Janosky J. Continuous intrathecal baclofen infusion for spasticity of cerebral origin. JAMA. 1993;270(20):2475–7.
6. McCall TD, MacDonald JD. Cervical catheter tip placement for intrathecal baclofen administration. Neurosurgery. 2006;59(3):634–40.
7. Sivakumar G, Yap Y, Tsegaye M, Vloeberghs M. Intrathecal baclofen therapy for spasticity of cerebral origin–does the position of the intrathecal catheter matter? Childs Nerv Syst. 2010;26(8):1097–102.
8. Saulino MF, Creamer MJ, Spencer R, Abouihia A, Saltuari L. Post-stroke upper extremity spasticity reduction with intrathecal baclofen: Associated factors in the sisters study population. Neuromodulation. 2019;22(3):E57.
9. Adesinasi W, Isom M, Anderson AM, et al. Ideal intrathecal baclofen delivery location depends on multiple factors: human study on catheter position. Neuromodulation. 2020;23(3):e43.
10. Konrad P, Isom M, Anderson AM, Page L. Intrathecal baclofen (ITB) delivery location and its effect on spasticity. Neuromodulation. 2018;21(3):e86–7.
11. Skalsky AJ, Fournier CM. Intrathecal baclofen bolus dosing and catheter tip placement in pediatric tone management. Phys Med Rehabil Clin N Am. 2015;26(1):89–93.
12. Brennan PM, Whittle IR. Intrathecal baclofen therapy for neurological disorders: a sound knowledge base but many challenges remain. Br J Neurosurg. 2008;22(4):508–19.
13. Heetla HW, Staal MJ, Proost JH, van Laar T. Clinical relevance of pharmacological and physiological data in intrathecal baclofen therapy. Arch Phys Med Rehabil. 2014;95(11):2199–206.
14. Albright AL, Turner M, Pattisapu JV. Best-practice surgical techniques for intrathecal baclofen therapy. J Neurosurg. 2006;104(4 Suppl):233–9.
15. Dan B, Motta F, Vles JS, et al. Consensus on the appropriate use of intrathecal baclofen (ITB) therapy in paediatric spasticity. Eur J Paediatr Neurol. 2010;14(1):19–28.
16. Plassat R, Perrouin Verbe B, Menei P, et al. Treatment of spasticity with intrathecal Baclofen administration: long-term follow-up, review of 40 patients. Spinal Cord. 2004;42(1):686–93.
17. Adesinasi W, Isom M, Anderson AM, Shults R, Saulino M, Page L, Konrad P. Ideal intrathecal baclofen (ITB) delivery location depends on multiple factors: human study on catheter position. Neuromodulation. 2020;23(3):e43.
18. Jacobs NW, Maas EM, Brusse-Keizer M, Rietman HJS. Effectiveness and safety of cervical catheter tip placement in intrathecal baclofen treatment of spasticity: a systematic review. J Rehabil Med. 2021;53(7):jrm00215. https://doi.org/10.2340/16501977-2857.
19. Page L, Konrad P, Adesinasi W, Isom MT, Anderson AM, Shults R. Baclofen drug distribution along the spinal axis: pharmacokinetic findings in a pilot human study. Neuromodulation. 2019;22(3):e236.
20. Armstrong MJ, Okun MS. Diagnosis and treatment of parkinson disease: a review. JAMA. 2020;323(6):548–60.

21. Barker R, Mason SL. The hunt for better treatments for Huntington's disease. Lancet. 2019;18(2):131–3.
22. Hardiman O, Al-Chalabi A, Chio A, Corr EM, Logroscino G, Robberecht W, Shaw PJ, Simmons Z, van den Berg LH. Amyotrophic lateral sclerosis. Nat Rev Dis Primers. 2017;3:17071.
23. Cook M, Murphy M, Bulluss K, D'Souza W, Plummer C, Priest E, Williams C, Sharan A, Fisher R, Pincus S, Distad E, Anchordoquy T, Abrams D. Anti-seizure therapy with a long-term, implanted intra-cerebroventricular delivery system for drug-resistant epilepsy: a first-in-man study. EClinical-Medicine. 2020;22:100326.
24. Hsu Y, Hettiarachchi HD, Zhu DC, Linninger AA. The frequency and magnitude of cerebrospinal fluid pulsations influence intrathecal drug distribution: key factors for interpatient variability. Anesth Analg. 2012;115(2):386–94.
25. Hettiarachchi HD, Hsu Y, Harris TJ Jr, Penn R, Linninger AA. The effect of pulsatile flow on intrathecal drug delivery in the spinal canal. Ann Biomed Eng. 2011;39(10):2592–602.
26. Hladky SB, Barrand MA. Mechanisms of fluid movement into, through and out of the brain: evaluation of the evidence. Fluids Barriers CNS. 2014;11(1):26.
27. Brinker T, Stopa E, Morrison J, Klinge P. A new look at cerebrospinal fluid circulation. Fluids Barriers CNS. 2014;11:10.
28. Deer TR, Pope JE, Hayek S et al. The Polyanalgesic Consensus Conference (PACC): Recommendations for Intrathecal Drug Delivery: Guidance for Improving Safety and Mitigating Risks. Neuromodulation. 2017;20(2):155–17.
29. Calias P, Papisov M, Pan J, Savioli N, Belov V, Huang Y, Lotterhand J, Alessandrini M, Liu N, Fischman AJ, Powell JL, Heartlein MW. CNS penetration of intrathecal-lumbar dursulfase in the monkey, dog and mouse: implications for neurological outcomes of lysosomal storage disorder. PLoS ONE. 2012;7(1):e30341.
30. Chung JK, Brown E, Crooker B, Palmieri KJ, McCauley TG. Biodistribution of idursulfase formulated for intrathecal use (idursulfase-IT) in cynomolgus monkeys after intrathecal lumbar administration. PLoS ONE. 2016;11(10):e0164765.
31. Xie H, Chung JK, Mascelli MA, McCauley TG. Pharmacokinetics and bioavailability of a therapeutic enzyme (idursulfase) in cynomolgus monkeys after intrathecal and intravenous administration. PLoS ONE. 2015;10(4):e0122453.
32. Tangen K, Nestorov I, Verma A, Sullivan J, Holt RW, Linninger AA. In-vivo intrathecal tracer dispersion in cynomolgus monkey validates wide biodistribution along neuraxis. IEEE Trans Biomed Eng. 2020;67(4):1122–32.
33. Sullivan JM, Mazur C, Wolf DA, Horky L, Currier N, Fitzsimmons B, Hesterman J, Pauplis R, Haller S, Powers B, Tayefeh L, DeBrosse–Serra B, Hoppin J, Kordasiewicz H, Swayze EE, Verma A. Convective forces increase rostral delivery of intrathecal radiotracers and antisense oligonucleotides in the cynomolgus monkey nervous system. J Transl Med. 2020;18:309.
34. Höfling SB, Hultsch C, Wester HJ, Heinrich MR. Radiochemical 18F-fluoroarylation of unsaturated α-, β- and γ-amino acids, application to a radiolabelled analogue of baclofen. Tetrahedron. 2008;64(52):11846–51.
35. Naik R, Valentine V, Dannals RF, Wong DF, Horti AG. Synthesis and evaluation of a new 18F-labelled radiotracer for studying the GABAB receptor in the mouse brain. ACS Chem Neurosci. 2018;9(6):1453–61.
36. Thakker D, Adams E, Stewart GR, Shafer LL. Distribution of molecules through the cerebral spinal fluid (CSF) of non-human primates: influence of delivery site, flow rate, and molecular mass of the test agent. Program No. 558.02/H7. 2011 Neuroscience Meeting Planner. Washington, DC:Society for Neuroscience, 2011. Online.
37. Page L, Bodner J, Egan B. Intrathecal drug dispersion: trialing vs chronic infusion. Neuromodulation. 2019;22(3):E262.
38. Nasser Z, Diana LL, Farzad S, Pablo OHJ, Alexandra C, Francisco TZJ. Deep brain stimulation and drug-resistant epilepsy: a review of the literature. Front Neurol. 2019;10:601.
39. Sass LR, Khani M, Romm J, Schmid Daners M, McCain K, Freeman T, et al. Non-invasive MRI quantification of cerebrospinal fluid dynamics in amyotrophic lateral sclerosis patients. Fluids Barriers CNS. 2020;17(1):4. https://doi.org/10.1186/s12987-019-0164-3.
40. Almutairi MM, Gong C, Xu YG, Chang Y, Shi H. Factors controlling permeability of the blood-brain barrier. Cell Mol Life Sci. 2016;73(1):57–77.
41. Simon MJ, Iliff JJ. Regulation of cerebrospinal fluid (CSF) flow in neurodegenerative, neurovascular and neuroinflammatory disease. Biochim Biophys Acta. 2016;1862(3):442–51.
42. Sanchez AL, Martinez-Bazan C, Gutierrez-Montes C, Criado-Hidalgo E, Pawlak G, Bradley w, Haughton V, Lasheras JC. On the bulk motion of the cerebrospinal fluid in the spinal canal. J Fluid- Mech. 2018;841:203–27.
43. Khani M, Braden JL, Sass LR, Gibbs CP, Pluid JJ, Oshinski JN, Stewart GR, Zeller JR, Martin BA. Characterization of intrathecal cerebrospinal fluid geometry and dynamics in cynomolgus monkeys (macaca fascicularis) by magnetic resonance imaging. PLoS ONE. 2019;14(2):e0212239.
44. McCully CML, Rodgers Lt, Garcia RC, Thomas ML, Peer CJ, Figg WD, Barnard DE, Warren KE. Flow rate and apparent volume of cerebrospinal fluid in Rhesus Macaques (Macaca mulatta) based on the pharmacokinetics of intrathecally administered inulin. Comp Med. 2020;70(6):526–31.

Publisher's Note